Send Orders for Reprints to reprints@benthamscience.ae

Doubly Thiocyanato(S,N)-Bridged Dinuclear Complexes of Mercury(II) from the Use of 2-pyridyl Oximes as Capping Ligands

Panagiota Danelli[1], Zoi G. Lada[1], Catherine P. Raptopoulou[2], Vassilis Psycharis[2,*], Theocharis C. Stamatatos[3,*] and Spyros P. Perlepes[1,4,*]

Vassilis Psycharis

[1]*Department of Chemistry, University of Patras, GR-265 04 Patras, Greece;* [2]*Institute of Nanoscience and Nanotechnology, NCSR "Demokritos", GR-153 10 Aghia Paraskevi Attikis, Greece;* [3]*Department of Chemistry, Brock University, L2S 3A1 St. Catharines, Ontario, Canada;* [4]*Institute of Chemical Engineering Sciences, Foundation for Research and Technology-Hellas (Forth/ICE-HT), Platani, P.O. Box 1414, GR-265 04 Patras, Greece*

Spyros P. Perlepes

T.C. Stamatatos

Abstract: The reactions between $Hg(SCN)_2$ and the 2-pyridyl oximes, 2-pyridine aldoxime (paoH), methyl 2-pyridyl ketone oxime (mepaoH), pyridine-2-amidoxime (NH_2paoH) and di-2-pyridyl ketone oxime (dpkoxH), have been investigated. The products in Me_2CO or Me_2CO/MeOH are the dinuclear complexes $[Hg_2(SCN)_4(paoH)_2]$ (**1**), $[Hg_2(SCN)_4(mepaoH)_2]$ (**2**), $[Hg_2(SCN)_4(NH_2paoH)_2]$ (**3**) and $[Hg_2(SCN)_4(dpkoxH)_2]$ (**4**), whose structures have been determined by single-crystal X-ray crystallography. The molecular structures consist of centrosymmetric dinuclear molecules in which the two Hg^{II} ions are bridged by two bidentate bridging $\eta^1{:}\eta^1{:}\mu$ ($\mu_{1,3}$) SCN^- groups forming a planar (**1**, **2**) or non-planar (**3**, **4**), 8-membered metallacyclic ring. The Hg^{II} centers are each chelated by a N(2-pyridyl), N(oxime)-bidentate ligand and are bound to one terminal S-bonded thiocyanato group. Due to the very long Hg^{II}-N (bridging SCN^-) distances in **3**, this complex can also be described as *pseudo*dimer. The second 2-pyridyl ring of each dpkoxH ligand in **4** remains uncoordinated. The 2D lattice of **1** and **2** is built through H-bonding and π-π stacking interactions. Hydrogen bonds and S**...**S interactions generate 3D networks in **3** and **4**. The IR spectra of the complexes are discussed in terms of the coordination modes of the ligands involved (SCN^-, 2-pyridyl oximes). ^{1}H NMR spectra in d_6-DMSO indicate that the complexes decompose in solution.

Keywords: Coordination chemistry, crystal structures, dinuclear mercury(II) complexes, ^{1}H NMR spectra, infrared spectroscopy, oxime group, 2-pyridyl oxime ligands, thiocyanato ligands.

1. INTRODUCTION

More than one century after the preparation and preliminary characterization of bis(dimethylglyoximato)nickel(II) by Chugaev, which was a landmark in inorganic gravimetric analysis, the chemistry of metal-oxime/oximate complexes continues to attract the intense interest of coordination, structural, supramolecular, analytical and physical chemists [1-3]. The interest arises from several reasons, ranging from the solution of pure chemical and spectroscopic problems to applied topics (catalysts, corrosion inhibition of Fe surfaces by oximes, metal recovery and detoxification using solvent extraction, etc.) and to aspects of metallosupramolecular chemistry and Molecular Magnetism [1-10]. Oxime and oximate groups can bind a metal ion [4] in several coordination modes shown in Fig. (**1**). *It is not an exaggeration to state that from the metals in the Periodic Table, the study of the reactions of mercury(I) and mercury(II) with oxime/oximate ligands has practically been neglected*; selected examples are provided in refs. [11] and [12].

*Address correspondence to these authors at the Department of Chemistry, University of Patras, GR-265 04 Patras, Greece;
Tel: +30 2610996730; Fax: +30 2610997118;
E-mails: perlepes@patreas.upatras.gr, tstamatatos@brocku.ca and vpsychar@ims.demokritos.gr

Ligands possessing one oxime group and one pyridyl moiety, with or without other donor sites, are popular in coordination chemistry. Most of these ligands contain a 2-pyridyl group and thus are named 2-pyridyl oximes (Fig. **2**). The anionic forms of these molecules are versatile ligands for a variety of research objectives, including μ, μ_3 and μ_4 behaviours [13, 14]. The activation of 2-pyridyl oximes by 3d-metal ions is also becoming a fruitful area of research [14, 15]. For many years, our groups have been engaged in the use of 2-pyridyl oxime/oximate and their isomeric ligands for the synthesis of 3d-, 4f- and 3d/4f-metal coordination complexes with emphasis on their magnetic or/and optical properties [16-30]. With the exception of the tetrahedral complex $[HgCl_2(paoH)]$ [31], where paoH is 2-pyridine aldoxime (R=H in Fig. **2**), *no mercury(II) or mercury(I) complexes of 2-pyridyl oximes have been reported so far.*

Because of its various applications in thermometers, diffusion pumps, batteries and dental amalgams, mercury is simultaneously neurotoxic in almost all of its forms and the expression "mad as a hatter" has been derived from the effects of $Hg(NO_3)_2$ poisoning to hat-makers who use this salt for the treatment of fur [32, 33]. The most dangerous form of mercury is the CH_3Hg^+ ion produced by anaerobic microbes [32-34], and the competition between methylation and de-

1877-945X/15 $58.00+.00 © 2015 Bentham Science Publishers

methylation (to inorganic forms of the element) controls concentrations in the environment [35]. As a consequence of the toxic effects of Hg(II), emphasis is currently placed on development of organic ligands that, selectively, either remove Hg^{II} from contaminated water using liquid- liquid (or solvent) extraction or respond to the presence of this metal ion through a change of one or more properties of the system (such as redox potentials, absorption or fluorescence spectra) [36-40].

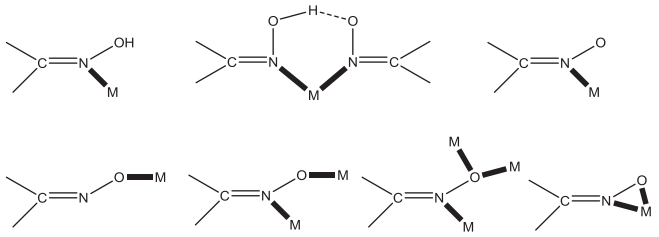

Fig. (1). The crystallographically established coordination modes of oxime and oximato groups; note that the upper central mode combines one formally neutral oxime and one formally anionic oximato group, as, for example, observed in bis(dimethylglyoximato)-nickel(II).

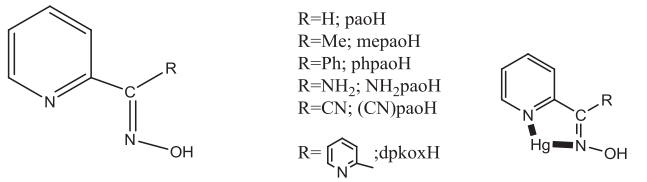

Fig. (2). General structural formula of 2-pyridyl oximes (left), abbreviations of some of them (middle) and the N,N'-bidentate chelating mode of the ligands observed in the mercury(II) complexes **1**-**4** (right). The ligands used in the present work are 2-pyridine aldoxime (IUPAC name: pyridine-2-carbaldehyde oxime; paoH), methyl 2-pyridyl ketone oxime (IUPAC name: 1-pyridin-2-yl-ethanone oxime; mepaoH), pyridine-2-amidoxime (IUPAC name: N-hydroxy-pyridine-2-carboxamidine; NH_2paoH) and di-2-pyridyl ketone oxime (IUPAC name: di-pyridin-2-yl-methanone oxime; dpkoxH).

We have recently embarked on a programme aiming at the amalgamation of the above mentioned two research topics, namely the use of 2-pyridyl oxime ligands in Hg(II) chemistry, in order to explore the influences of the ligands' substituents (R in Fig. **2**) and the inorganic anions that are present in the Hg(II) starting materials on the product identity. The short- term goals of our project are the access of new structural types of Hg(II) complexes, the study of their spectroscopic properties (e.g. fluorescence) and the investigation of Hg^{II}-mediated reactions of the oxime group. Our long-term goal is the investigation of the possibility to use lipophilic 2-pyridyl oximes (i.e. ligands in which R consists of aromatic rings or aliphatic chains with many carbon atoms) for the solvent extraction of Hg(II) from waste waters, as it is the case for the toxic Cd(II) [41]. We report here the products formed from the reactions between $Hg(SCN)_2$ and the 2-pyridyl oximes paoH, mepaoH, NH_2paoH and dpkoxH (for their structural formulae, common and IUPAC names, see Fig. **2**). The ligands paoH and mepaoH contain only two donor sites, i.e. the 2-pyridyl nitrogen atom and the oxime group (which has two potential donor sites with the O-ligation being favoured upon oxime deprotonation). Characteristics that differentiate the R groups in NH_2paoH and dpkoxH (R= NH_2 and 2-pyridyl ring, respectively; Fig. **2**) in comparison with the R groups in paoH and mepaoH (R= H and Me, respectively; Fig. **2**) are the coordination capability, potential for deprotonation (only for NH_2paoH) and ability for hydrogen bonding formation in the former two.

2. EXPERIMENTAL

2.1. General and Physical Measurements

All manipulations were performed under aerobic conditions using reagents and solvents (Alfa Aesar, Aldrich) as received. The ligands 2-pyridine aldoxime (paoH) and di-2-pyridyl ketone oxime (dpkoxH) are commercially available. The ligands methyl 2-pyridyl ketone oxime (mepaoH) and pyridine-2-amidoxime (NH_2paoH) were synthesized *via* the reaction of the appropriate ketone with hydroxylamine as described in the literature [42-44]. Carbon, hydrogen and nitrogen microanalyses were performed by the Instrumental Analysis Laboratory of the University of Patras (Greece). IR spectra in the 4000-400 cm^{-1} region were recorded using a Perkin-Elmer 16PC FT-IR spectrometer; the samples were in the form of KBr pellets prepared under pressure. The ^1H NMR spectra of the free ligands and their mercury(II) complexes were recorded using a 400 MHz Bruker Avance DPX spectrometer; tetramethylsilane was used as the internal standard.

2.2. Syntheses

2.2.1. $[Hg_2(SCN)_4(paoH)_2]$ (1)

A solution of $Hg(SCN)_2$ (0.063 g, 0.20 mmol) in Me_2CO (9 mL) was added to a solution of paoH (0.054 g, 0.44 mmol) in the same solvent (1 mL). The resulting colourless solution was stirred for a further 5 min and filtered. Vapour diffusion of Et_2O into the reaction solution gave colourless crystals of the product after 3-4 days. The crystals were collected by filtration, washed with cold Me_2CO (1 mL) and Et_2O (2x5 mL), and dried in a vacuum desiccator over $CaCl_2$. The yield was 40% (based on the Hg^{II} available). Anal. Calcd for $C_{16}H_{12}Hg_2N_8O_2S_4$: C, 21.90; H, 1.38; N, 12.77%. Found: C, 21.63; H, 1.42; N, 12.74%. IR data (KBr, cm^{-1}): 3560 (mb), 3180 (wb), 3092 (wb), 2998 (w), 2900 (w), 2806 (w), 2140 (m), 2110 (s), 1616 (m), 1594 (m), 1566 (w), 1508 (m), 1434 (m), 1320 (m), 1306 (m), 1218 (w), 1158 (w), 1020 (s), 982 (m), 940 (w), 886 (m), 778 (s), 738 (m), 670 (m), 632 (m), 518 (m), 490 (w), 432 (w), 402 (w). ^1H NMR data (d_6-DMSO, δ/ppm): 11.80 (s, 1H), 8.61 (d, 1H), 8.17 (s, 1H), 7.89 (t, 1H), 7.80 (d, 1H), 7.45 (t, 1H).

2.2.2. $[Hg_2(SCN)_4(mepaoH)_2]$ (2)

A solution of $Hg(SCN)_2$ (0.063 g, 0.20 mmol) in Me_2CO (8 mL) was added to a solution of mepaoH (0.054 g, 0.40 mmol) in the same solvent (1 mL). The resulting colourless solution was layered with Et_2O (18 mL) and stored at 4 ^oC. Slow diffusion gave X-ray quality crystals of the product after 10 days. The crystals were collected by filtration, washed with cold Me_2CO (0.5 mL) and Et_2O (2x5 mL), and dried in a vacuum desiccator over $CaCl_2$. The yield was 45%

(based on the Hg^{II} available). Anal. Calcd for $C_{18}H_{16}Hg_2N_8O_2S_4$: C, 23.87; H, 1.78; N, 12.37%. Found: C, 23.69; H, 1.77; N, 12.68%. IR data (KBr, cm^{-1}): 3440 (mb), 3148 (mb), 3082 (w), 2920 (w), 2852 (w), 2120 (s), 1638 (w), 1592 (m), 1566 (w), 1478 (m), 1436 (w), 1370 (w), 1322 (m), 1292 (w), 1252 (w), 1162 (w), 1132 (m), 1094 (w), 1058 (sh), 1034 (s), 776 (s), 740 (w), 676 (m), 450 (w), 434 (w), 406 (w). ^{1}H NMR data (d_6-DMSO, δ/ppm): 11.78 (s, 1H), 8.63 (d, 1H), 7.89 (t, 2H), 7.47 (ddd, 1H), 2.25 (s, 3H).

2.2.3. [Hg$_2$(SCN)$_4$(NH$_2$paoH)$_2$] (3)

A solution of $Hg(SCN)_2$ (0.063 g, 0.20 mmol) in Me_2CO (10 mL) was added to an almost colourless solution of NH_2paoH (0.055 g, 0.40 mmol) in MeOH (4 mL). A small quantity of a black solid was precipitated. The reaction mixture was stirred for a further 10 min and filtered to remove the black precipitate. Vapour diffusion of Et_2O into the colourless filtrate gave well-formed, X-ray quality crystals of the product after 15 days. The crystals were collected by filtration, washed with cold MeOH (1 mL) and Et_2O (2x5 mL), and dried in a vacuum desiccator over $CaCl_2$. The yield was 24%. Anal. Calcd for $C_{16}H_{14}Hg_2N_{10}O_2S_4$: C, 21.18; H, 1.55; N, 15.43%. Found: C, 21.38; H, 1.57; N, 15.54%. IR data (KBr, cm^{-1}): 3434 (s), 3344 (m), 3185 (mb), 3086 (w), 2882 (w), 2112 (s), 1658 (s), 1612 (m), 1594 (s), 1568 (m), 1490 (m), 1478 (sh), 1412 (m), 1392 (m), 1300 (w), 1174 (w), 1158 (w), 1096 (m), 1014 (m), 940 (s), 832 (m), 786 (s), 738 (m), 684 (m), 634 (w), 476 (mb), 448 (w), 404 (w). ^{1}H NMR data (d_6-DMSO, δ/ppm): 10.15 (sb, 1H), 8.57 (d, 1H), 7.90 (mt, 2H), 7.47 (t, 1H), 6.09 (sb, 2H).

2.2.4. [Hg$_2$(SCN)$_4$(dpkoxH)$_2$] (4)

A solution of $Hg(SCN)_2$ (0.063 g, 0.20 mmol) in Me_2CO (4 mL) was slowly added to a solution of dpkoxH (0.080 g, 0.40 mmol) in the same solvent (14 mL). The resulting pale yellow solution was stirred for a further 5 min and stored in the fridge. X-ray quality, colourless crystals of the product were precipitated after 2 days, which were collected by filtration, washed with cold Me_2CO (2 mL) and Et_2O (2x5 mL), and dried in a vacuum desiccator over $CaCl_2$. Typical yields were in the range 30-35% (based on the Hg^{II} available). Anal. Calcd for $C_{26}H_{18}Hg_2N_{10}O_2S_4$: C, 30.26; H, 1.76; N, 13.58%. Found: C, 30.01; H, 1.90; N, 13.23%. IR data (KBr, cm^{-1}): 3420 (mb), 3098 (w), 3045 (w), 2895 (w), 2118 (s), 1634 (w), 1590 (m), 1564 (w), 1472 (m), 1432 (w), 1384 (w), 1332 (w), 1282 (w), 1242 (w), 1200 (w), 1154 (w), 1098 (w), 1056 (m), 1034 (sh), 1008 (s), 956 (m), 902 (w), 786 (s), 750 (m), 688 (m), 656 (w), 630 (m), 498 (w), 460 (w), 436 (w), 414 (w), 404 (w). ^{1}H NMR data (d_6-DMSO, δ/ppm): 11.94 (sb, 1H), 8.61 (d, 1H), 8.48 (d, 1H), 7.88-7.86 (mt, 2H), 7.79 (d, 1H), 7.53 (d, 1H), 7.42-7.39 (dt, 2H).

2.3. Single-crystal X-ray Crystallography

Crystals of **1** (0.18x 0.60x 0.64 mm), **2** (0.07x 0.12x 0.19 mm), **3** (0.17x 0.23x 0.47 mm) and **4** (0.07x 0.17x 0.48 mm) were taken from the mother liquor and immediately cooled to -113 ^{o}C. Single-crystal X-ray data were collected on a Rigaku R-AXIS SPIDER Image Plate diffractometer; the radiation was the graphite-monochromated Cu Kα. The collection and processing of the data were carried out using the package of the CrystalClear program [45]. The solution and refinement (full-matrix least-squares techniques on F^2) of the structures were performed by SHELXS-97 and SHELXL-97, respectively [46]. All non-hydrogen atoms were refined using anisotropic thermal parameters, while hydrogen atoms were either introduced at calculated positions or located in difference Fourier maps. Graphics were drawn using the package of the Diamond 3 program [47]. Unit cell parameters and structure solution and refinement data are listed in Table **1**. Further crystallographic details for **1**: $2\theta_{max}$= 130^o; reflections collected/unique/used, 12584/1781 (R_{int}= 0.1266)/1781; 162 parameters refined; $(\Delta/\sigma)_{max}$= 0.001; $(\Delta\rho)_{max}/(\Delta\rho)_{min}$= 1.567/-2.848 e/Å^3; R_1/wR_2 (for all data), 0.0464/0.1170. Further crystallographic details for **2**: $2\theta_{max}$= 130^o; reflections collected/unique/used, 11645/1898 (R_{int}= 0.0858)/1898; 156 parameters refined; $(\Delta/\sigma)_{max}$= 0.001; $(\Delta\rho)_{max}/(\Delta\rho)_{min}$= 1.455/-1.755 e/Å^3; R_1/wR_2 (for all data), 0.0419/0.0923. Further crystallographic details for **3**: $2\theta_{max}$= 130^o; reflections collected/unique/used, 13019/1856 (R_{int}= 0.1088)/1856; 172 parameters refined; $(\Delta/\sigma)_{max}$= 0.001; $(\Delta\rho)_{max}/(\Delta\rho)_{min}$= 2.217/-2.211 e/Å^3; R_1/wR_2 (for all data), 0.0415/0.0996. Further crystallographic details for **4**: $2\theta_{max}$= 130^o; reflections collected/unique/used, 17937/2464 (R_{int}= 0.0734)/2464; 230 parameters refined; $(\Delta/\sigma)_{max}$= 0.001; $(\Delta\rho)_{max}/(\Delta\rho)_{min}$= 1.147/-1.452 e/Å^3; R_1/wR_2 (for all data), 0.0365/0.0806. Full details can be found in the deposited CIF files, CCDC 1039896-1039899.

3. RESULTS AND DISCUSSION

3.1. Synthesis Comments

In the present study, we have investigated the reactions between the 2-pyridyl oximes paoH, mepaoH, NH_2paoH, dpkoxH (Fig. **2**), and $Hg(SCN)_2$ *in the absence of external bases*; Hg^{II}/SCN^- complexes with these ligands were unknown in the literature. A variety of $Hg(SCN)_2$/2-pyridyl oxime reaction systems involving different reagent ratios, solvent media and crystallization methods were systematically employed for a given ligand in arriving at the optimized procedures described in Section 2.2. Reactions of $Hg(SCN)_2$ and paoH, mepaoH, dpkoxH in 1:2 to 1:2.5 molar ratios in Me_2CO afforded solutions from which were subsequently isolated complexes $[Hg_2(SCN)_4(paoH)_2]$ (**1**), $[Hg_2(SCN)_4(mepaoH)_2]$ (**2**), $[Hg_2(SCN)_4(dpkoxH)_2]$ (**4**), respectively, in moderate yields (30-45%). For the crystallization of $[Hg_2(SCN)_4(NH_2paoH)_2]$ (**3**), MeOH had to be added in the reaction solution. The Me_2CO/MeOH solvent mixture caused the precipitation of a black solid (most probably HgS), which was removed by filtration before crystallization of the product. The stoichiometric, i.e. 1:1, reactions give again the same products (as revealed by elemental analyses, and IR and ^{1}H NMR spectra), albeit in lower yields. Assuming that the dinuclear compounds are the only products from their respective reaction mixtures, the preparation of **1**-**4** can be represented by Eq. (1), where LH= paoH, mepaoH, NH_2paoH, dpkoxH. The addition of external bases, e.g. Et_3N or NaOMe, in the reaction systems gives thiocyanate-free (IR evidence) complexes which have not been crystallized to date.

$$2\,Hg(SCN)_2 + 2\,LH \xrightarrow[Me_2CO/\,MeOH\,(\mathbf{3})]{Me_2CO\,(\mathbf{1},\,\mathbf{2},\,\mathbf{4})} [Hg_2(SCN)_4(LH)_2] \quad \mathbf{1\text{-}4}$$

Table 1. Crystallographic data for complexes 1-4.

Parameter	1	2	3	4
Formula	$C_{16}H_{12}Hg_2N_8O_2S_4$	$C_{18}H_{16}Hg_2N_8O_2S_4$	$C_{16}H_{14}Hg_2N_{10}O_2S_4$	$C_{26}H_{18}Hg_2N_{10}O_2S_4$
Formula weight	877.76	905.81	907.79	1031.92
Crystal system	Triclinic	Triclinic	Triclinic	Orthorhombic
Space group	*P* -1	*P* - 1	*P* - 1	*Pbca*
a (Å)	7.2476(1)	7.3420(1)	7.3089(1)	10.2125(2)
b (Å)	8.3455(2)	8.1569(2)	7.4713(1)	14.4721(3)
c (Å)	10.5246(2)	11.4428(2)	12.1817(2)	20.6758(4)
α (°)	74.862(1)	73.820(1)	76.622(1)	90.00
β (°)	81.473(1)	77.994(1)	85.784(1)	90.00
γ (°)	72.721(1)	70.981(1)	71.050(1)	90.00
V (Å^3)	585.03(2)	617.01(2)	612.08(2)	3055.81(11)
Z	1	1	1	4
T (°C)	-113	-113	-113	-113
Radiation	Cu Kα	Cu Kα	Cu Kα	Cu Kα
ρ_{calcd} (g cm^{-3})	2.491	2.438	2.463	2.243
μ (mm^{-1})	26.822	25.462	25.694	20.704
Reflections with $I > 2\sigma(I)$	1732	1784	1805	2265
$R_1{}^a$ ($I > 2\sigma(I)$)	0.0457	0.0397	0.0405	0.0332
$wR_2{}^b$ ($I > 2\sigma(I)$)	0.1164	0.0903	0.0975	0.0785

$^aR_1 = \Sigma(||F_o|-|F_c||)/\Sigma(|F_o|)$. $^bwR_2 = \{\Sigma[w(F_o^2-F_c^2)]/\Sigma[w(F_o^2)^2]\}^{1/2}$, $w = 1/[\sigma^2(F_o^2) + (aP)^2 + bP]$, where $P = [\max(F_o^2, 0) + 2F_c^2]/3$ (*a*= 0.0667 and *b*= 2.8881 for **1**; *a*= 0.0414 and *b*= 1.2846 for **2**; *a*= 0.0454 and *b*= 1.7493 for **3**; *a*= 0.0243 and *b*= 8.2010 for **4**).

3.2. Description of Structures

Various structural plots for complexes **1-4** are shown in Figs. (**3**)-(**11**). Selected interatomic distances and angles are listed in Tables **2** and **3**, while hydrogen bonding details are presented in Table **4**. The coordination mode of the neutral 2-pyridyl oximes in complexes **1-4** is illustrated in Fig. (**2**), right.

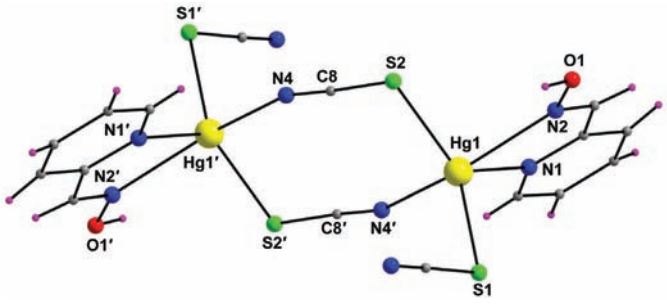

Fig. (3). Partially labeled plot of the structure of the dinuclear molecule that is present in complex **1**. Primed and unprimed atoms are related by the crystallographic inversion center (symmetry operation: 1-*x*, -*y*, 2-*z*). Colour code for the electronic version of the paper: Hg^{II} yellow, S green, N blue, O red, C grey, H purple.

The molecular structures of complexes **1**, **2** and **4** are very similar and thus only the structure of **1** will be described in detail. The structure consists of dinuclear $[Hg_2(SCN)_4(paoH)_2]$ molecules (Fig. **3**). There is a crystallographically imposed inversion center at the midpoint of the Hg1**...**Hg1′ distance. The Hg^{II} centers are bridged by a pair of *syn*, *syn*-η^1:η^1:μ (or 2.11 using Harris notation) SCN^- groups. The Hg^{II} ions are each chelated by a N(pyridyl), N′(oxime)- bidentate paoH ligand (η^1:η^1 or 1.11). A terminal S-bonded (i.e. thiocyanato) ligand completes five-coordination at each metal center. The metal coordination geometry can be described as very distorted square pyramidal; the basal plane consists of donor atoms N2, N4′, S1 and S2, and the 2-pyridyl nitrogen atom N1 occupies the apical position. The alternative distorted trigonal bipyramidal description of the coordination geometry places donor atoms N2 and N4′at the axial positions and atoms S1, S2 and N1 at the equatorial positions. The distortions from regular geometry are partly attributed to the d^{10} nature of Hg^{II} (zero crystal field stabilization energy with no preference to a particular geometry) and the small bite angle of the 5-membered chelating ring (N1-Hg1-N2= 67.7°). The Hg-N(2-pyridyl) bond is stronger than the Hg-N(oxime) bond, the Hg1-N1 and Hg1-N2 bond lengths being 2.362(8) and 2.534(7) Å,

Table 2. Selected interatomic distances (Å) and angles (°) for complexes 1 and 2[a, b].

Distance	Complex 1	Complex 2	Angle	Complex 1	Complex 2
Hg1...Hg1′	6.102(1)	6.179(1)	N1-Hg1-N2	67.7(3)	67.5(2)
Hg1-N1	2.362(8)	2.356(7)	N1-Hg1-S1	105.1(2)	104.6(2)
Hg1-N2	2.534(7)	2.486(6)	N1-Hg1-S2	120.7(2)	118.9(2)
Hg1-S1	2.467(3)	2.461(2)	N1-Hg1-N4′	83.7(3)	82.6(2)
Hg1-S2	2.463(2)	2.455(2)	N2-Hg1-S1	102.2(2)	112.1(2)
Hg1-N4′	2.580(8)	2.812(6)	N2-Hg1-S2	90.4(2)	93.7(2)
N2-O1	1.387(9)	1.397(8)	N2-Hg1-N4′	148.3(3)	149.3(2)
N4-C8[c]/C9[d]	1.139(12)	1.154(9)	S1-Hg1-S2	133.8(1)	135.5(1)
C8[c]/C9[d]- S2	1.667(9)	1.657(8)	S1-Hg1-N4′	98.2(2)	81.4(2)
			S2-Hg1-N4′	92.8(2)	94.7(2)
			N4- C8[c]/C9[d]-S2	176.0(7)	177.3(7)

[a] Primed and unprimed atoms for complex **1** are related by the symmetry operation 2-*x*, -*y*, 2-*z*. [b] Primed and unprimed atoms for complex **2** are related by the symmetry operation -*x*, 1-*y*, 1-*z*. [c] For complex **1** (Fig. **3**). [d] For complex **2** (Fig. **4**).

respectively. Somewhat to our surprise, the Hg-S(terminal SCN^-) and Hg-S(bridging SCN^-) bond distances are very similar. The 8-membered Hg1-($\mu_{1,3}$-SCN)$_2$-Hg1′ ring, formed by the two metal ions and the two head-to-tail bridging SCN^- groups, is almost planar, the maximum deviation from the mean plane of the eight atoms being 0.046 Å for N4 (and its symmetry equivalent) (Fig. **4**). Both terminal and bridging SCN ligands are almost linear.

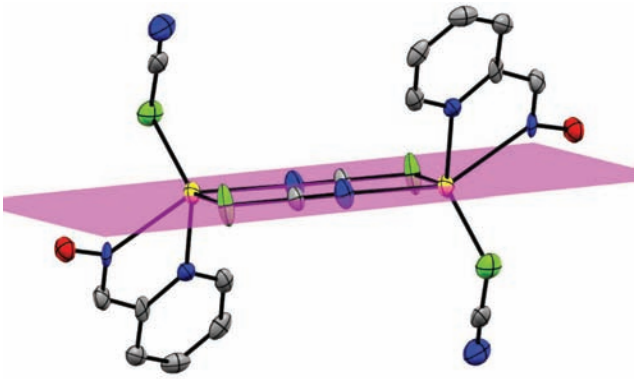

Fig. (4). A drawing that shows the planarity of the 8-membered Hg1-($\mu_{1,3}$-SCN)$_2$-Hg1′ ring in complex **1**. Colour code for the electronic version of the paper: Hg^{II} yellow, S green, N blue, O red, C grey.

The Hg1-($\mu_{1,3}$-SCN)$_2$-Hg1′ metallacyclic ring is also almost planar in complex **2** (Fig. **5**; maximum deviation from the mean plane is 0.165 Å for N4 and N4′), but it deviates significantly from planarity in complex **4** (Fig. **6**; atoms N5, C13, S2, Hg1 and their symmetry equivalents are 0.559, 0.111, 0.552 and 0.510 Å from the best mean plane through the eight atoms). The second 2-pyridyl ring (i.e. that containing N3) of dpkoxH in complex **4** is uncoordinated and the angle between the two planes is 71.8°. The metal coordination geometry in **4** cannot be described in two ways (square pyramidal or trigonal bipyramidal); its best description is as distorted square pyramidal, with the 2-pyridyl nitrogen atom N1 at the apex of the pyramid.

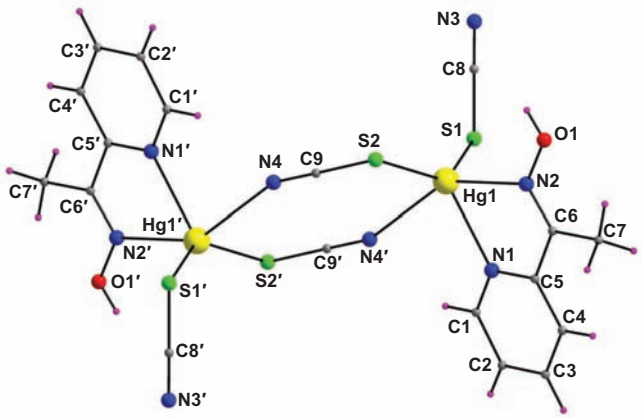

Fig. (5). Fully labeled plot of the structure of the centrosymmetric dinuclear molecule that is present in complex **2**. Primed and unprimed atoms are related by the crystallographic inversion center (symmetry operation: -*x*, 1-*y*, 1-*z*). Colour code for the electronic version of the paper: Hg^{II} yellow, S green, N blue, O red, C grey, H purple.

The structure of complex **3** can be described in two ways. Adopting the first description, the structure consists of distorted tetrahedral [Hg(SCN)$_2$(NH$_2$paoH)] molecules with S-bonded SCN^- groups; the mononuclear molecules are in close contact to form a centrosymmetric pair. According to the second description (which is illustrated in Fig. **7**), the structure consists of centrosymmetric *pseudo*dinuclear [Hg$_2$(SCN)$_4$(NH$_2$paoH)$_2$] molecules with very weakly bonding Hg1**...**N5′ (and Hg1′**...**N5) interactions of 3.058(8) Å. Adopting the second description, Hg1 (and Hg1′) is 5-coordinate with a very distorted square pyramidal geometry which places N2 (and N2′) at the apical position; the

Table 3. Selected interatomic distances (Å) and angles (°) for complexes 3 and 4[a, b].

Distance	Complex 3	Complex 4	Angle	Complex 3	Complex 4
Hg1···Hg1′	5.467(1)	5.626(1)	N1-Hg1-N2	68.5(3)	65.9(1)
Hg1-N1	2.375(7)	2.367(4)	N1-Hg1-S1	102.8(2)	106.9(1)
Hg1-N2	2.340(8)	2.645(4)	N1-Hg1-S2	113.0(2)	105.3(1)
Hg1-S1	2.446(2)	2.410(2)	N1-Hg1-N5′[d]/N5[e]	137.3(2)	87.3(1)
Hg1-S2	2.430(2)	2.437(2)	N2-Hg1-S1	111.1(2)	107.4(1)
Hg1-N5′[d]/N5[e]	3.058(8)[c]	2.635(5)	N2-Hg1-S2	110.7(2)	83.7(1)
N2-O1	1.401(10)	1.378(6)	N2-Hg1- N5′[d]/N5[e]	69.3(2)	148.1(2)
N5-C8[d]/C13′[e]	1.127(1)	1.143(7)	S1-Hg1-S2	132.4(1)	147.7(1)
C8[d]/C13′[e]- S2[d]/S2′[e]	1.690(6)	1.678(6)	S1-Hg1- N5′[d]/N5[e]	86.6(2)	96.3(1)
			S2-Hg1- N5′[d]/N5[e]	87.6(2)	87.5(1)
			N5- C8[d]/C13′[e]-S2[d]/S2′	177.2(7)	178.0(6)

[a] Symmetry operation for primed atoms in complex **3**: 1-*x*, 1-*y*, 1-*z*. [b] Symmetry operation for primed atoms in complex **4**: 1-*x*, -*y*, -*z*. [c] This distance may represent a weak bonding interaction (see text). [d] For complex **3** (Fig. **5**). [e] For complex **4** (Fig. **6**).

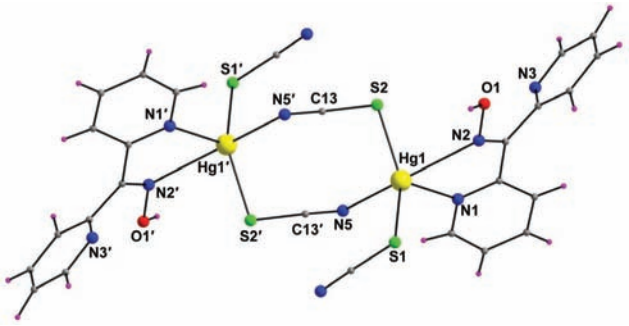

Fig. (6). Partially labeled plot of the structure of the dinuclear molecule that is present in complex **4**. Primed and unprimed atoms are related by the crystallographic inversion center (symmetry operation: 1-*x*, -*y*, -*z*). Colour code for the electronic version of the paper: Hg^{II} yellow, S green, N blue, O red, C grey, H purple.

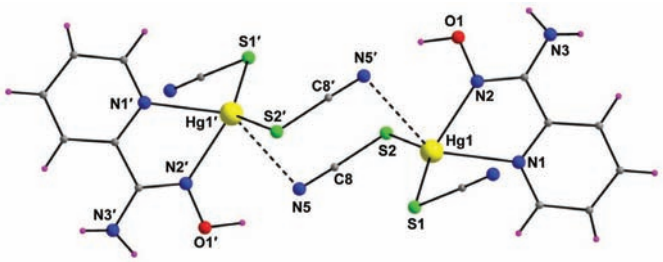

Fig. (7). Partially labeled plot of the structure of the *pseudo*dinuclear molecule that is present in complex **3**. Primed and unprimed atoms are related by the crystallographic inversion center (symmetry operation: 1-*x*, 1-*y*, 1-*z*). The Hg1**...**N5′ and Hg1′**...**N5′ distances of 3.058(8) Å (dashed lines) can be considered as very weakly bonding interactions. Colour code for the electronic version of the paper: Hg^{II} yellow, S green, N blue, O red, C grey, H purple.

Hg1-($\mu_{1,3}$-SCN)$_2$-Hg1′ 8-membered ring is not planar, the deviations of the eight atoms from their mean plane being in the range 0.059-0.861 Å.

The Hg^{II}**...**Hg^{II} distances in **1**-**4** are in the range 5.467(1)-6.179(1) Å (Tables **2** and **3**). This variation can be partly attributed to the different orientations of the strictly parallel (by symmetry) orientations of the linear bridging SCN^- groups with respect to the metal-metal axis. If we take the C(bridging SCN^-)-S(bridging SCN^-)-Hg1 and C(bridging SCN^-)-N(bridging SCN^-)-Hg1 bond angles as measures of this orientation, we can observe that, in general, as these two bond angles decrease, the metal**...**metal distance also decreases. For example, in **1** the Hg1**...**Hg1′ distance is 6.102(1) Å and the C8-S2-Hg1 and C8-N4-Hg1′ angles are 103.1(3) and 159.8(6)°, respectively, whereas in **4** the Hg1**...**Hg1′ distance is 5.626(1) Å and the C13-S2-Hg1 and C13-N5′-Hg1′ angles are 97.6 (2) and 123.1(5)°, respectively. Complex **2** (Hg1**...**Hg1′= 6.179(1) Å) does not fit well within this trend and a possible reason is the large Hg1-N4′ distance of 2.812(6) Å.

We have up to now discussed the molecular structures of **1**-**4**. The crystal structures of these complexes are also interesting. The lattice structure of **1** (Fig. **8**) is built through H-bonding (Table **4**) and π-π stacking interactions. The dinuclear molecules are linked through intermolecular O1-H1O**...**N3 (N3 is the uncoordinated nitrogen atom of the terminal thiocyanato ligand that is not labeled in Fig. **3**) hydrogen bonds forming 1D chains which are further linked through π-π interactions developed between the 2-pyridyl rings of paoH to create a 2D network that extends parallel to the (110) plane. The centroid-centroid distance between the symmetry-related rings is 3.545 Å.

H-bonding and π-π stacking interactions are also present in the lattice structure of **2** (Fig. **9** and Table **4**). The hydrogen bond that links the dimers into 1D chains parallel to the *c* axis is of the same type with that in **1**, i.e. the donor is the uncoordinated oxime oxygen atom and the acceptor is the uncoordinated nitrogen atom of the terminal thiocyanato ligand. The chains are further linked through π-π interactions

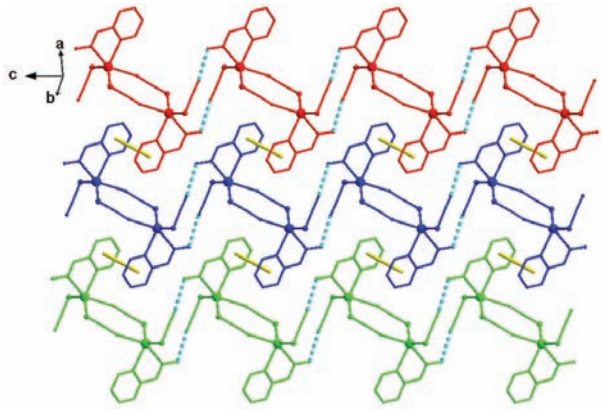

Fig. (8). A small part of the 2D-network structure of **1** due to H-bonding (cyan dashed lines for the electronic version of the paper) and π-π stacking interactions (yellow lines for the electronic version of the paper). Three chains, formed by hydrogen bonds, are shown in different colours.

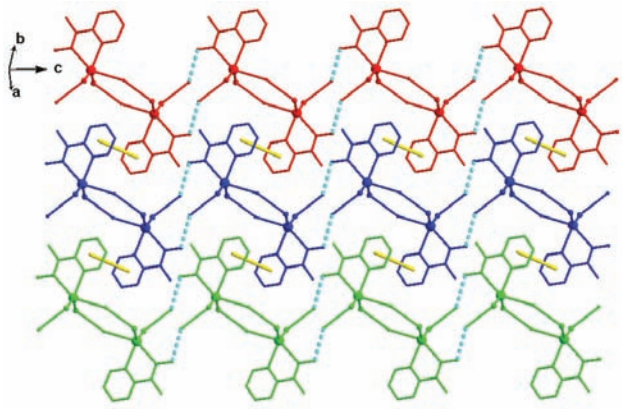

Fig. (9). A small part of the 2D network that is present in the crystal structure of **2**, formed through H-bonding (cyan dashed lines for the electronic version of the paper) and π-π stacking interactions (yellow lines for the electronic version of the paper). Three chains, formed by hydrogen bonds, are shown in different colours.

Table 4. Hydrogen bonds in the structures of complexes 1-4[a].

Interaction	D...A (Å)	H...A (Å)	D-H...A (°)	Symmetry operation
Complex **1**				
O1-H1O...N3[b]	2.711	1.881	169.5	2-*x*, -*y*, 1-*z*
Complex **2**				
O1-H1O...N3	2.706	1.872	171.9	-*x*, 1-*y*, 2-*z*
Complex **4**				
O1-H1O...N3	2.668	1.953	177.0	0.5+*x*, *y*, 0.5-*z*
Complex **3**				
O1-H1O...N5′[c]	2.737	1.776	151.7	1-*x*, 1-*y*, 1-*z*
N3-HA(N3)...O1	3.015	2.274	139.5	1-*x*, 1-*y*, -*z*
N3-HB(N3)...N4[d]	3.037	2.181	138.7	2-*x*, 1-*y*, -*z*

[a] Abbreviations: A= acceptor; D= donor. [b] N3 is the "free" (i.e. uncoordinated) nitrogen atom of the terminal thiocyanato ligand (not labeled in Fig. **3**). [c] Intradimer hydrogen bond. [d] N4 is the "free" (i.e. uncoordinated) nitrogen atom of the terminal thiocyanato ligand (not labeled in Fig. **7**).

between the 2-pyridyl rings of the mepaoH ligands to create a 2D network extending parallel to the (110) plane (as in **1**); the centroid-centroid distance between the symmetry-related 2-pyridyl rings is 3.931 Å.

The lattice structure of **4** (Fig. **10**) is built through H-bonding interactions (Table **4**) and S**...**S contacts. The dinuclear molecules are linked through intermolecular hydrogen bonds involving the oxime oxygen atom as donor and the nitrogen atom of the uncoordinated 2-pyridyl ring of dpkoxH as acceptor; these hydrogen bonds create a 2D network that extends parallel to the (010) plane. The 2D sheets are further linked through intermolecular S1**...**S2 (1.5-*x*, -0.5+*y*, *z*) contacts at 3.831 Å along the *b* axis to build an overall 3D framework.

In the structure of **3** there are three different, crystallographically independent hydrogen bonds. Considering the complex as consisting of *pseudo*dimers (Fig. **7**), the O1-H1O**...**N5′ hydrogen bond (Table **4**) can be described as intramolecular; this involves the oxime oxygen atom as donor and the nitrogen atom of the *pseudo*bridging SCN^- group as acceptor. The amino functionality is responsible for the formation of two intermolecular hydrogen bonds, acting as donor; the acceptors are the oxime oxygen atom and the "free" (i.e. uncoordinated) nitrogen atom of the terminal SCN^- group that is not labeled in Fig. (**7**). These two intermolecular hydrogen bonds form a 2D network which extends parallel to the (010) plane (Fig. **11**, left). The 2D layers are further linked through intermolecular S1**...**S2 (*x*, 1+*y*, *z*) contacts at 3.679 Å building an overall 3D framework (Fig. **11**, right).

Complexes **1**-**4** are the *first* $Hg(SCN)_2$/2-pyridyl oxime complexes. As mentioned in Introduction, only one Hg(II) complex with a 2-pyridyl oxime ligand has been structurally characterized, namely the monomeric tetrahedral compound $[HgCl_2(paoH)]$ [31]. Compounds **1**, **2** and **4** join a handful of structurally characterized dinuclear Hg(II) complexes containing the $\{\eta^1\text{-}\underline{S}CN)Hg(\eta^1{:}\eta^1{:}\mu\text{-}SCN)_2Hg(\eta^1\text{-}\underline{S}CN)\}$ unit

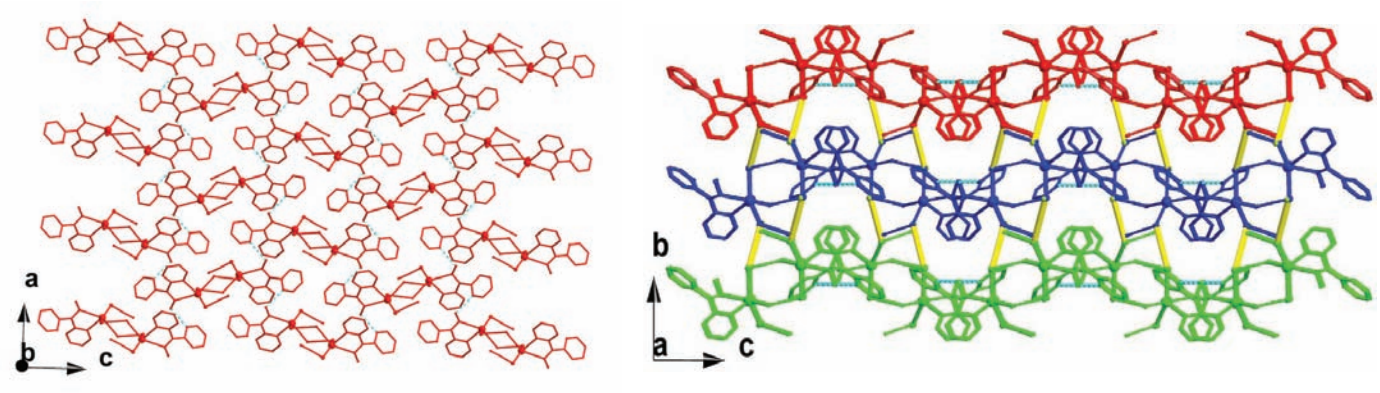

(a) **(b)**

Fig. (10). (**a**) A small part of the 2D network in the crystal structure of **4**, formed through O1-H1O**...**N3 hydrogen bonds (cyan dashed lines for the electronic version of the paper). (**b**) A small part of the 3D framework in **4** due to intermolecular S1**...**S2 contacts (yellow lines for the electronic version of the paper), showing three 2D layers in different colours.

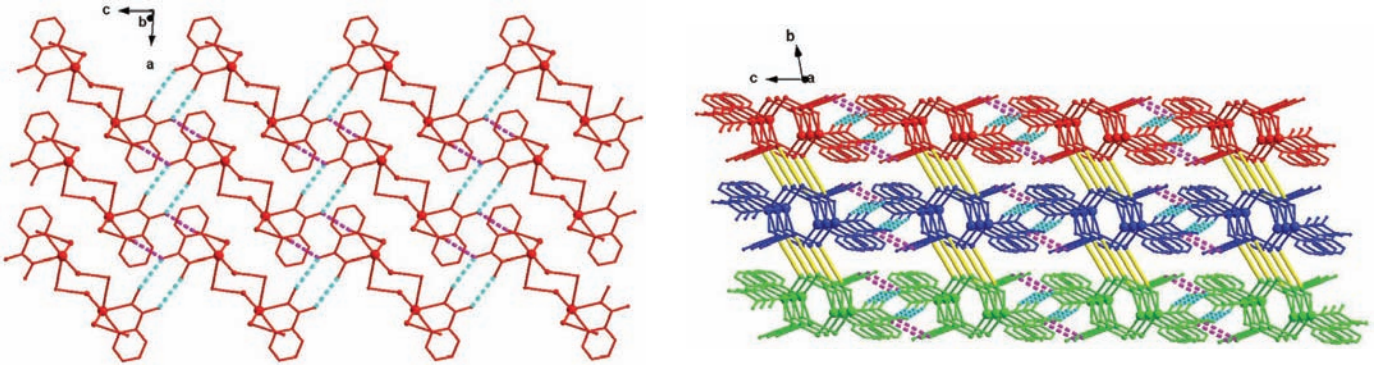

(a) **(b)**

Fig. (11). (**a**) A small part of the 2D network in the crystal structure of **3**, formed through two intermolecular hydrogen bonds (cyan and magenta dashed lines for the electronic version of the paper) involving the amino functionality as donor. (**b**) A small part of the 3D framework in **3** due to intermolecular S1**...**S2 contacts (yellow lines for the electronic version of the paper), showing three 2D layers in different colours.

[48-52]. This unit is also present in polymeric complexes containing bis-bidentate bridging ligands [53]. The *pseudo*dimeric nature of **3** has never been observed in complexes of $Hg(SCN)_2$ with bidentate chelating ligands.

3.3. Spectroscopic Studies

The IR spectrum of the representative complex **4** is shown in Fig. (**12**). The presence of the neutral oxime group in complexes **1**-**4** is manifested by a broad IR band at 3560-3185 cm^{-1}, assigned to $\nu(OH)_{oxime}$ [23, 26, 54]. Their broadness and relatively low wavenumber are both indicative of hydrogen bonding. The strong bands at 3464 and 3348 cm^{-1} in the IR spectrum of free NH_2paoH are assigned to the $\nu_{as}(NH_2)$ and $\nu_s(NH_2)$ modes, respectively [55]. The absence of large shifts of these bands in the spectrum of **3** (they appear at 3434 and 3344 cm^{-1}, respectively) implies that there is no interaction between the amino group and the Hg^{II} center [55]. The in-plane deformation of the 2-pyridyl ring of free paoH, mepaoH and NH_2paoH (at 627, 632 and 596 cm^{-1}, respectively) shift upwards in the spectra of **1**-**3** (at 670, 676 and 634 cm^{-1}, respectively) confirming the involvement of the ring-N atom in coordination [23, 26, 55]. The appearance of three bands in the 630-690 cm^{-1} in the spectrum of **4** might reflect the presence of both uncoordinated and coordinated 2-pyridyl rings in this compound. Many bands appear in the 1660-1380 cm^{-1} region in the IR spectra of the complexes. Contributions from the $\nu(C{=}N)_{oxime}$, $\delta(OH)$, $\delta(NH_2)$, $\delta(CH_3)$ and aromatic ring stretching vibrations would be expected in this region, rendering exact assignments and discussion of the coordination shifts impossible. The medium-intensity band at 985 cm^{-1} in the spectrum of free paoH has been assigned to the $\nu(NO)_{oxime}$ vibration [26]; in the spectrum of the paoH-containing complex **1**, this mode appears at almost the same wavenumber (982 cm^{-1}). The absence of shift is in accord with the fact that the N-O bond length of the neutral paoH ligand in **1** (1.387(9) Å) is the same with that in the free paoH molecule (1.391 Å) [26].

The IR spectra of **1**, **2**, **3** and **4** exhibit very strong bands at 2140/2110, 2120, 2112 and 2118 cm^{-1}, respectively, assigned [56] to the carbon-nitrogen stretching vibration, ν(CN), of the SCN^- group. These wavenumbers are in the typical region observed for S-bonded (M-SCN) and bridging (M-SCN-M) SCN^- ligands [56]. The stretching frequency of a bridging group is generally higher than that of a terminal S-bonded group [56]. Since the four complexes under study contain both bridging and S-bonded terminal SCN^- groups, we would expect two ν(CN) bands. The appearance of two bands is clearly observed only in the spectrum of **1** (2140 and 2110 cm^{-1}). The higher frequency band is assigned to the ν(CN) mode of the bridging SCN^- group, whereas the lower

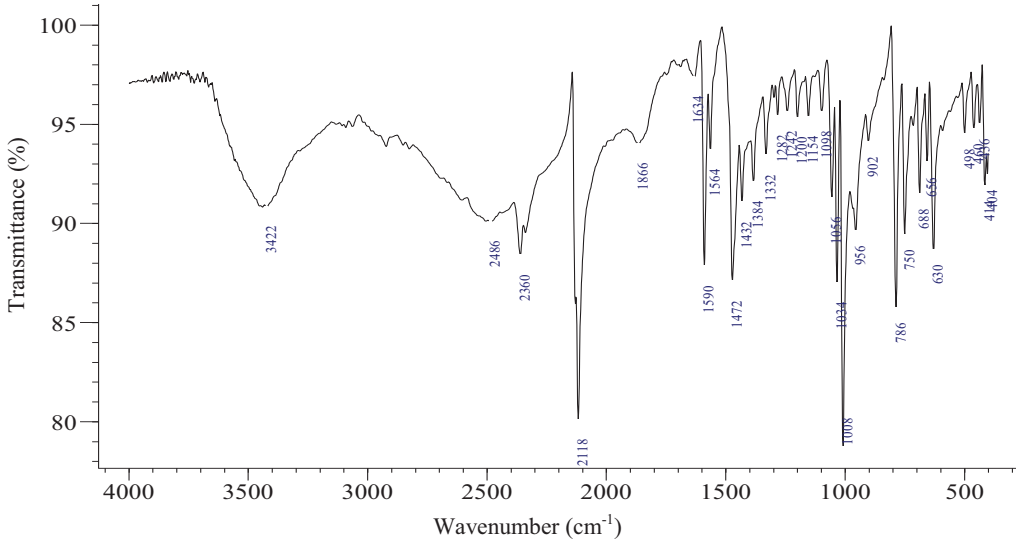

Fig. (12). The IR spectrum of complex $[Hg_2(SCN)_4(dpkoxH)_2]$ (**4**).

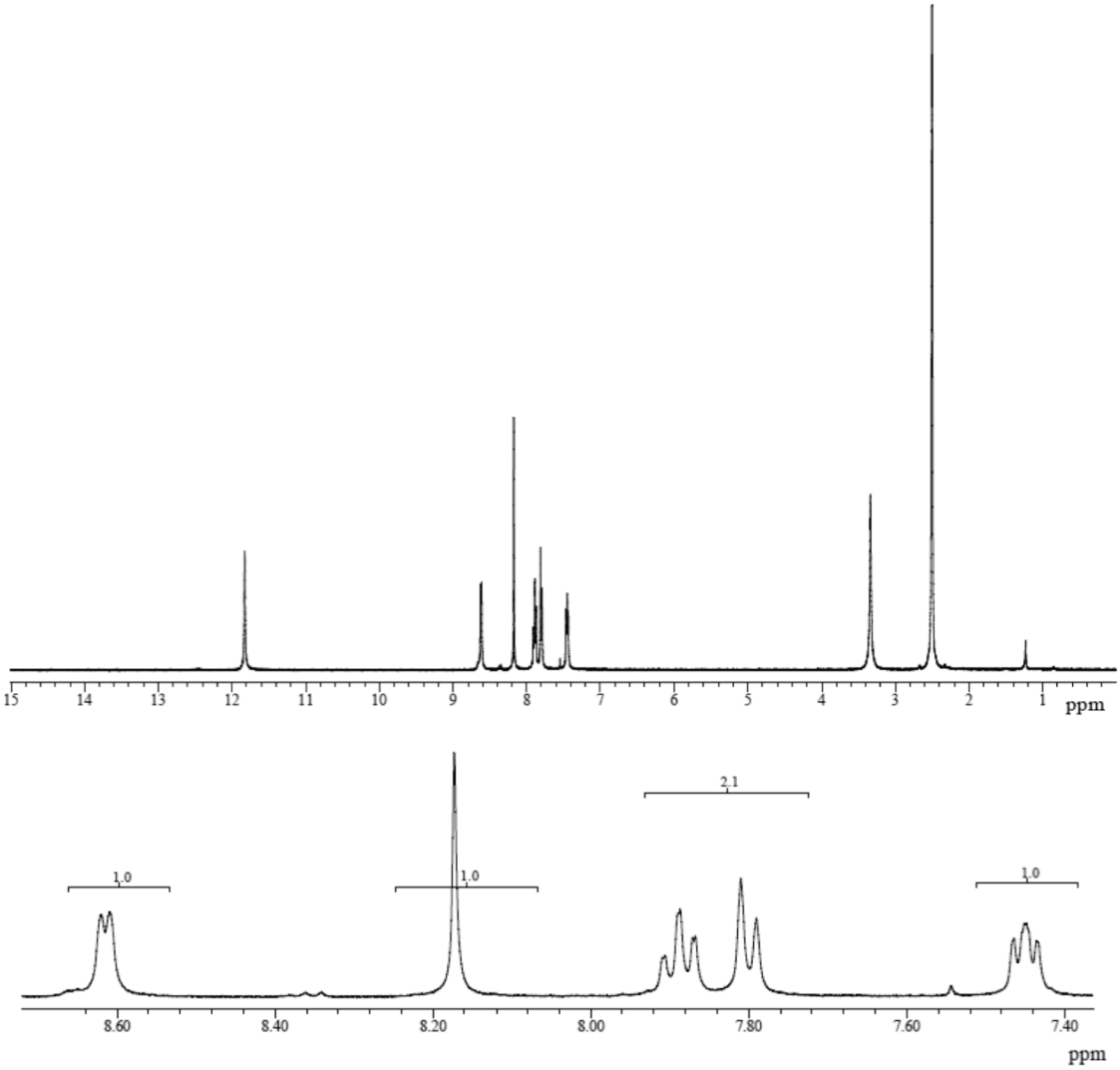

Fig. (13). (top) The ^{1}H NMR spectrum of complex $[Hg_2(SCN)_4(paoH)_2]$ (**1**) in d_6-DMSO in the δ 15-0 ppm region. (bottom) ^{1}H NMR signals of complex **1** in the δ region 8.75-7.40 ppm. The signal at 2.50 ppm is due to the methyl groups of the non-deuterated amount of the solvent, while the signal at 3.34 ppm is attributed to the protons of the H_2O content of the solvent.

Table 5. Diagnostic ^{1}H NMR data[a] for the free ligands paoH, mepaoH, NH_2paoH, dpkoxH and their metal complexes 1-4.

Compound	=NO-H	6-pyridyl[b]	HC=N-[c]	-CH_3	-NH_2
paoH	11.62(s)	8.57(d)	8.08(s)	-	-
1	11.80(s)	8.61(d)	8.17(s)	-	-
mepaoH	11.50(s)	8.58(d)	-	2.21(s)	-
2	11.78(s)	8.63(d)	-	2.25(s)	-
NH_2paoH	9.86(s)	8.55(d)	-	-	5.84(sb)
3	10.15(sb)	8.57(d)	-	-	6.09(sb)
dpkoxH	11.81(s)	8.58(d), 8.43(d)	-	-	-
4	11.94(sb)	8.61(d), 8.48(d)	-	-	-

[a] In d_6-DMSO at 400 Hz; chemical shifts (δ values) are given in ppm relative to Me_4Si (spectra recorded at room temperature). [b] The proton attached to the aromatic carbon atom that is *ortho* to the ring-N atom; dpkoxH and **4** possess two such protons because they contain two pyridyl rings. [c] This is the proton attached to the oxime carbon atom. b= broad; d=doublet; s=singlet.

frequency band reflects the simultaneous presence of S-bonded terminal, thiocyanato group in the complex [56]. Thus, it is evident that the two types of SCN^- ligands in **1**-**4** cannot be differentiated by IR spectroscopy. The ν(CS) and δ(NCS) modes of the SCN^- ligands, expected in the 680-740 and 420-480 cm^{-1} regions, respectively, could not be assigned in an unambiguous way because these bands are weak and tend to be obscured by other bands [56].

The solubilities of **1**-**4** in common "inert" organic solvents were too low to allow other than d_6-DMSO solutions to be prepared and studied. The ^{1}H NMR spectrum of the representative complex **1** is shown in Fig. (**13**). In general, the chemical shifts of coordinated ligand protons bound to diamagnetic metal ions are influenced by three factors [54]: (i) the electron density on the ligand (especially in the region near the coordination sites) diminishes upon coordination, inducing downfield shifts; (ii) steric effects lead to downfield shifts; and (iii) alignment of a proton above an adjacent aromatic ring leads to an upfield shift. Diagnostic ^{1}H NMR chemical shifts of complexes **1**-**4** are given in Table **5**.

The ^{1}H NMR spectra of the complexes are very similar (but not superimposable) with the spectra of their respective free ligands recorded under the same experimental conditions. This is a strong evidence (but not definite proof) that the complexes decompose in solution with possible formation of $Hg^{II}/SCN^-/d_6$-DMSO species (the Hg^{II}-S_{DMSO} bond is thermodynamically stable) and release of free ligands. It should be mentioned that a downfield shift is observed for the oxime proton resonance in the spectra of the complexes (relative to the signal of this proton for the corresponding free ligand), in agreement with a greater acidity of the oxime group in the complexes; however, this downfield shift is smaller than that expected if coordination of the oxime nitrogen persists in solution [54]. Also a greater downfield shift for the 6-pyridyl proton(s) of the complexes would be observed if coordination of the ring-N atom occurred.

CONCLUSIONS AND PERSPECTIVES

The first use of four 2-pyridyl oximes in Hg^{II}/SCN^- chemistry has provided access to interesting dinuclear complexes containing the rare {(SCN)Hg($\mu_{1,3}$-SCN)$_2$Hg(SCN)} unit and one chelating N(pyridyl), N(oxime)-ligand per metal ion. The crystal (i.e. supramolecular) structures of the complexes are also interesting. The combination of H-bonding and π-π stacking interactions lead to 2D networks in **1** and **2**, while H-bonding and S**…**S interactions generate 3D networks in **3** and **4**.

We have no reason to believe that this research theme is exhausted of new interesting results. We are currently targeting products from the HgX_2/ 2-pyridyl oximes general reaction systems (X= Cl, Br, I, NO_3, ClO_4, $MeCO_2$, $PhCO_2$) with the goal to investigate their structural types. The coordination chemistry of 2,6-pyridyl dioximes (e.g. 2,6-diacetylpyridine dioxime and pyridine-2,6-diamidoxime) with Hg(II) is unknown and we are studying reactions of these tridentate chelating ligands with all mercury(II) starting materials that are available. The ability of paoH, mepaoH, NH_2paoH and dpkoxH to undergo deprotonation and act as anionic ligands bridging two or three metal ions gives us hopes for the isolation of high-nuclearity Hg(II) oximate coordination clusters and the preparation of mixed-metal mercury(II)/lanthanide(III) complexes with interesting magnetic and/or optical properties.

CONFLICT OF INTEREST

The authors confirm that this article content has no conflict of interest.

ACKNOWLEDGEMENTS

This research was co-financed by the European Union (European Social Fund- ESF) and Greek National Funds through the Operational Program "Education and Lifelong Learning" of the National Strategic Reference Framework (NSRF)- Research Funding Program: THALES. Investing in Knowledge society through the European Social Fund. This work was also supported by NSERC Discovery Grant (to Th. C. S.).

SUPPLEMENTARY INFORMATION

CCDC 1039896- 1039899 contain the supplementary crystallographic data for complexes **1**-**4**. These data can be

obtained free of charge via http://www.ccdc.cam.ac.uk/conts/retrieving.html or from the Cambridge Crystallographic Data Centre, 12 Union Road, Cambridge CB2 1EZ, UK; fax: (+44) 1223-336033; or e-mail: deposit@ccdc.cam.ac.uk.

REFERENCES

[1] Kukushkin, V. Yu.; Tudela, D.; Pombeiro, A. J. L. Metal-ion assisted reactions of oximes and reactivity of oxime-containing metal complexes. *Coord. Chem. Rev.*, **1996**, *156*, 333-362.

[2] Kukushkin, V. Yu.; Pombeiro, A. J. L. Oxime and oximate complexes: unconventional synthesis and reactivity. *Coord. Chem. Rev.*, **1999**, *181*, 147-175.

[3] Gerasimchuk, N.; Maher, T. Tin(IV) cyanoximates: Synthesis, characterization and cytoxicity. *Inorg. Chem.*, **2007**, *46*, 7268-7284.

[4] Pombeiro, A. J. L.; Kukushkin, V. Yu. In: *Comprehensive Coordination Chemistry II*, J. A. McCleverty and T. J. Meyer, Ed.; Elsevier; Amsterdam, **2004**; Vol. 1, pp. 631-637.

[5] Kopylovich, M. N.; Kukushkin, V. Yu.; Haukka, M.; Fraüsto da Silva, J. J. R.; Pombeiro, A. J. L. Zinc(II)/Ketoxime system as a simple and efficient catalyst for hydrolysis of organonitriles. *Inorg. Chem.*, **2002**, *41*, 4798-4804.

[6] Thorpe, J. M.; Beddoes, R. L.; Collison, D.; Garner, C. D.; Helliwell, M.; Holmes, J. M.; Tasker, P. A. Surface coordination chemistry: Corrosion inhibitors by tetranuclear cluster formation of iron with salicylaldoximes. *Angew. Chem. Int. Ed.*, **1999**, *38*, 1119-1121.

[7] Tasker, P. A.; Tong, C. C.; Westra, A. N. Co-extraction of cations and anions in base metal recovery. *Coord. Chem. Rev.*, **2007**, *251*, 1868-1877.

[8] Smith, A. G.; Tasker, P. A.; White, D. J. The structures of phenolic oximes and their complexes. *Coord. Chem. Rev.*, **2003**, *241*, 61-85.

[9] Koumousi, E. S.; Routzamani, A.; Nguyen, T. N.; Giannopoulos, D. P.; Raptopoulou, C. P.; Psycharis, V.; Christou, G.; Stamatatos, Th. C. 2-Pyrrolyloximes in high-nuclearity transition-metal cluster chemistry: Fe_{10} and Fe_{12}. *Inorg. Chem.*, **2013**, *52*, 1176-1178.

[10] Milios, C. J.; Winpenny, R. E. P. Cluster-based single molecule magnets. *Struct. Bond.*, **2014**, in press (doi: 10.1007/430_2014_149).

[11] Nockemann, P.; Meyer, G. Mercurous dimethylglyoximato nitrate, $Hg_2(Dmg)_2(NO_3)_2$. *Z. Anorg. Allg. Chem.*, **2003**, *629*, 931-932.

[12] Biswas, S.; Sarkar, S.; Steele, I. M.; Sarkar, S.; Mostafa, G.; Bhaumik, B. B.; Dey, K. Two-dimensional supramolecular assembly of phenylmercury(II) and cadmium(II) complexes with a tridentate thiohydrazone NNS donor ligand: Synthesis, coordination behaviour and crystal structure. *Polyhedron*, **2007**, *26*, 5061-5068.

[13] Milios, C. J.; Stamatatos, Th. C.; Perlepes, S. P. The coordination chemistry of pyridyl oximes. *Polyhedron*, **2006**, *25*, 134-194.

[14] Chaudhuri, P. Homo- and hetero-polymetallic exchange coupled metal-oximates. *Coord. Chem. Rev.*, **2003**, *243*, 143-190.

[15] Konidaris, K. F.; Polyzou, C. D.; Kostakis, G. E.; Tasiopoulos, A. J.; Roubeau, O.; Teat, S. J.; Manessi-Zoupa, E.; Powell, A. K.; Perlepes, S. P. Metal ion- assisted transformations of 2-pyridinealdoxime and hexafluorophosphate. *Dalton Trans.*, **2012**, *41*, 2862-2865.

[16] Konidaris, K. F.; Giouli, M.; Raptopoulou, C. P.; Psycharis, V.; Verginadis, I. I.; Vasiliadis, A.; Afendra, A. S.; Karkabounas, S.; Manezzi-Zoupa, E.; Stamatatos, Th. C. Employment of pyridyl oximes and dioximes in zinc(II) chemistry: Synthesis, structural and spectroscopic characterization, and biological evaluation. *Inorg. Chim. Acta*, **2013**, *396*, 49-59.

[17] Alexandropoulos, D. I.; Mowson, A. M.; Pilkington, M.; Bekiari, V.; Christou, G.; Stamatatos, Th. C. Emissive molecular nanomagnets: Introducing optical properties in triangular oximato $\{Mn^{III}_3\}$ SMMs from the deliberate replacement of simple carboxylate ligands with their fluorescent analogues. *Dalton Trans.*, **2014**, *43*, 1965-1969.

[18] Milios, C. J.; Kefalloniti, E.; Raptopoulou, C. P.; Terzis, A.; Escuer, A.; Vicente, R.; Perlepes, S. P. 2-Pyridinealdoxime [(py)CHNOH] in manganese(II) carboxylate chemistry: Mononuclear, dinuclear, tetranuclear and polymeric complexes, and partial transformation of (py)CHNOH to picolinate (-1). *Polyhedron*, **2004**, *23*, 83-95.

[19] Stamatatos, Th. C.; Dionyssopoulou, S.; Efthymiou, G.; Kyritsis, P.; Raptopoulou, C. P.; Terzis, A.; Vicente, R.; Escuer, A.; Perlepes, S. P. The first cobalt metallacrowns: Preperation and characterization of mixed-valence cobalt(II/III), inverse 12-metallocrown-4 complexes. *Inorg. Chem.*, **2005**, *44*, 3374-3376.

[20] Stamatatos, Th. C.; Bell, A.; Cooper, P.; Terzis, A.; Raptopoulou, C. P.; Heath, S. L.; Winpenny, R. E. P. Old ligands with new coordination chemistry: Linear trinuclear mixed oxidation state cobalt(III/II/III) complexes and their mononuclear "ligand" cobalt(III) complexes featuring 2-pyridyloximates. *Inorg. Chem. Commun.*, **2005**, *8*, 533-538.

[21] Stamatatos, Th. C.; Pringouri, K. V.; Raptopoulou, C. P.; Vicente, R.; Psycharis, V.; Escuer, A.; Perlepes, S. P. An unusual dichromium(II, II) compound bearing di-2-pyridyl Ketone oximate ligands and prepared by the ligand-assisted reduction of a trichromium(III, III, III) complex in air. *Inorg. Chem. Commun.*, **2006**, *9*, 1178-1182.

[22] Stamatatos, Th. C.; Vlahopoulou, J. C.; Sanakis, Y.; Raptopoulou, C. P.; Psycharis, V.; Boudalis, A. K.; Perlepes, S. P. Formation of the $\{Cu^{II}_3(\mu_3\text{-}OH)\}^{5+}$ core in copper(II) carboxylate chemistry via use of di-2-pyridyl ketone oxime $[(py)_2CNOH]$: $[Cu_3(OH)(O_2CR)_2\{(py)_2CNO\}_3]$ (R= Me, Ph). *Inorg. Chem. Commun.*, **2006**, *9*, 814-818.

[23] Stoumpos, C. C.; Stamatatos, Th. C.; Sartzi, H.; Roubeau, O.; Tasiopoulos, A. J.; Nastopoulos, V.; Teat, S.J.; Christou, G.; Perlepes, S. P. Employment of methyl 2-pyridyl ketone oxime in manganese non-carboxylate chemistry: $Mn^{II}_2Mn^{IV}$ and $Mn^{II}_2Mn^{III}_6$ complexes. *Dalton Trans.*, **2009**, 1004-1015.

[24] Konidaris, K. F.; Kaplanis, M.; Raptopoulou, C. P.; Perlepes, S. P.; Zoupa-Manessi, E.; Katsoulakou, E. Dinuclear versus trinuclear complex formation in zinc(II) benzoate/pyridyl oxime chemistry depending on the position of the oxime group. *Polyhedron*, **2009**, *28*, 3243-3250.

[25] Escuer, A.; Vlahopoulou, G.; Perlepes, S. P.; Mautner, F. A. Trinuclear, tetranuclear and polymeric Cu^{II} complexes from the first use of 2-pyridylcyanoxime in trasition metal chemistry: Synthetic, structural and magnetic studies. *Inorg. Chem.*, **2011**, *50*, 2468-2478.

[26] Polyzou, C. D.; Lada, Z. G.; Terzis, A.; Raptopoulou, C. P.; Psycharis, V.; Perlepes, S. P. The fac diastereoisomer of tris-(2-pyridinealdoximato)cobalt(III) and a cationic cobalt(III) complex contatining both the neutral and anionic forms of the ligand: Synthetic, structural and spectroscopic studies. *Polyhedron*, **2014**, *79*, 29-36.

[27] Dermitzaki, D.; Raptopoulou, C. P.; Psycharis, V.; Escuer, A.; Perlepes, S. P.; Stamatatos, Th. C. Unexpected metal-ion assisted transformations leading to unexplored bridging ligands in Ni^{II} coordination chemistry: The case of PO_3F^{2-} group. *Dalton Trans.*, **2014**, *43*, 14520-14524.

[28] Polyzou, C. D.; Efthymiou, C. G.; Escuer, A.; Cuhna-Silva, L.; Papatriantafyllopoulou, C.; Perlepes, S. P. In search of 3d/4f- metal single-molecule magnets: Nickel(II)/lanthanide(III) coordination clusters. *Pure Appl. Chem.*, **2013**, *85*, 315-327.

[29] Polyzou, C. D.; Nikolaou, H.; Papatriantafyllopoulou, C.; Psycharis, V.; Terzis, A.; Raptopoulou, C. P.; Escuer, A.; Perlepes, S. P. Employment of methyl 2-pyridyl Ketone oxime in 3d/4f-metal chemistry: Dinuclear nickel(II)/lanthanide(III) species and complexes containing the metals in separate ions. *Dalton Trans.*, **2012**, *41*, 13755-13764.

[30] Konidaris, K. F.; Bekiari, V.; Katsoulakou, E.; Raptopoulou, C. P.; Psycharis, V.; Manessi-Zoupa, E.; Kostakis, G. E.; Perlepes, S. P. Investigation of the zinc(II)- benzoate-2-pyridinealdoxime reaction system. *Dalton Trans.*, **2012**, *41*, 3797-3806.

[31] Torabi, A. A.; Kian, R.; Suldozi, A.; Welter, R. Crystal structure of dichloro(pyridine-2-aldoxime-N,N') mercury(II), $HgCl_2(NC_5H_4CHNOH)$. *Z. Kristallogr. NCS*, **2005**, *220*, 613-614.

[32] Blum, J. D. Mesmerized by mercury. *Nature Chem.*, **2013**, *5*, 1066.

[33] Housecroft, C. E.; Sharpe, A. G. *Inorganic Chemistry*, 3rd ed.; Pearson: London, **2008**; p.748.

[34] Blum, J. D. Marine mercury breakdown. *Nature Geosci.*, **2011**, *4*, 139-140.

[35] Parks, J. M.; Johs, A.; Podar, M.; Bridou, R.; Hurt, Jr., R. A.; Smith, S. D.; Tomanicek, S. J.; Qian, Y.; Brown, S. D.; Brandt, C. C.; Palumbo, A. V.; Smith, J. C.; Wall, J. D.; Elias, D. A.; Liang, L. The genetic basis for bacterial mercury methylation. *Science*, **2013**, *339*, 1332-1335.

[36] Prodi, L.; Bargossi, C.; Montalti, M.; Zaccheroni, N.; Su, N.; Bradshaw, J. S.; Izatt, R. M.; Savage, P. B. An effective fluorescent chemosensor for mercury ions. *J. Am. Chem. Soc.*, **2000**, *122*, 6769-6770.

[37] Rurack, K.; Kollmannsberger, M.; Resch- Genger, U.; Daub, J. A selective and sensitive fluoroionophore for Hg^{II}, Ag^{I}, and Cu^{II} with virtually decoupled fluorophore and receptor units. *J. Am. Chem. Soc.*, **2000**, *122*, 968-969.

[38] Karagöz, F.; Güney, O.; Kandaz, M.; Bilgicli, A. T. Acridine-derivated receptor for selective mercury binding based on chelation- enhanced fluorescence effect. *J. Lumin.*, **2012**, *132*, 2736-2740.

[39] Babu, S. V.; Reddy, K. H. Direct spectrophotometric determination of mercury(II) using 2-acetylpyridine thiosemicarbazone in enviromental samples. *Indian J. Adv. Chem. Sci.*, **2012**, *1*, 65-72.

[40] Li, J.; Lu, W.; Ma, J.; Chen, L. Determination of mercury(II) in water samples using dispersive liquid- liquid microextraction and back extraction along with capillary zone electrophoresis. *Microchim. Acta*, **2011**, *175*, 301-308.

[41] Parus, A.; Wieszczycka, K.; Olszanowski, A. Solvent extraction of cadmium(II) from chloride solutions by pyridyl ketoximes. *Hydrometallurgy*, **2011**, *105*, 284-289.

[42] Orama, M.; Saarinen, H.; Korvenranta, J. Formation of trinuclear copper(II) complexes with three pyridine oxime ligands in aqueous solution. *J. Coord. Chem.*, **1990**, *22*, 183-190.

[43] Riggle, K.; Lynde-Kernell, T.; Schlemper, E.O. Synthesis and X-ray structures of Ni(II) complexes of 1-(2-pyridinyl)ethanone oxime. *J. Coord. Chem.*, **1992**, *25*, 117-125.

[44] Bernasek, E. Pyridinealdoximes. *J. Org. Chem.*, **1957**, *22*, 1263.

[45] *CrystalClear*, Rigaku/MSc Inc, The Woodlands, Texas, USA, **2005**.

[46] Sheldrick, G. M. A short history of SHELX. *Acta Crystallogr. A*, **2008**, *64*, 112-122.

[47] *Diamond*, Crystal and molecular structure visualization, ver. 3.1, Crystal Impact, Rathausgasse 30, 53111, Bonn, Germany.

[48] Gallagher, J. F.; Alyea, E. C.; Ferguson, G. Structural studies of steric effects in phosphine complexes: Dimers of bis{dithiocyanato(1-phenyldibenzophosphole) mercury(II)} associate with significant Hg-N nad Hg-S interdimer interactions. *Croat. Chem. Acta*, **1999**, *72*, 243-250.

[49] Lou, S.-F.; Wang, Q; Ding, J. Crystal structure of bis{[4,4,5,5-tetramethyl-2-(1-methyl-1H-benzimidazol-2-yl)-4.5-dihydroimidazole-1-oxyl-3-oxide-κ^2N,O](μ_2-thiocyanato-N:S)(thiocyanato-κS)mercury(II)}, $Hg_2(C_{15}H_{19}N_4O_2)_2(SCN)_4$. *Z. Kristallogr. NCS.*, **2012**, *227*, 105-106.

[50] Wang, E.-C.; Li, J.; Li, Y.-L.; Yang, E.-C.; Zhao, X.-J. Three 2-aminobenzothiazole-based mercury complexes tuned by competitive coordination between the coligands: Synthesis, structures, and fluorescent properties. *Synth. React. Inorg. Met.-Org. Nano-Met. Chem.*, **2011**, *41*, 791-797.

[51] Esmhosseini, M.; Safari, N.; Amani, V. Crystal structure of [hydroxy-methoxy-di(2-pyridyl)methane-κ^2N,N′]-(μ_2-thiocyanato-N:S)(thiocyanato-κS)mercury(II)}, $Hg(C_{12}H_{12}N_2O_2)_2(SCN)_2$. *Z. Kristallogr. NCS*, **2011**, *226*, 541-542.

[52] Padron, D. A.; Klausmeyer, K. K. Syntheses and coordination studies of 2-(diphenylphosphinomethyl)pyridine and its oxide towards mercury(II). *Polyhedron*, **2012**, *34*, 215-220.

[53] Mahmoudi, G.; Morsali, A. Three new Hg^{II} metal-organic polymers generated from 1,4-bis(n-pyridyl)-3,4-diaza-2,4-hexadiene ligands. *Inorg. Chim. Acta*, **2009**, *362*, 3238-3246.

[54] Koumousi, E.; Zampakou, M.; Raptopoulou, C. P.; Psycharis, V.; Beavers, C. M.; Teat, S. J.; Psomas, G.; Stamatatos, Th. C. First palladium(II) and platinum(II) complexes from employment of 2,6-diacetylpyridine dioxime: Synthesis, structural and spectroscopic characterization, and biological evaluation. *Inorg. Chem.* **2012**, *51*, 7699-7710.

[55] Nikolaou, H.; Terzis, A.; Raptopoulou, C. P.; Psycharis, V.; Bekiari, V.; Perlepes, S. P. Unique dinuclear, tetrakis(nitrato-O,O′)-bridged lanthanide(III) complexes from the use of pyridine-2-amidoxime: Synthesis, structural studies and spectroscopic characterization. J. Surface Interfaces Mater., **2015**, in press.

[56] Nakamoto, K. Infrared and Raman spectra of inorganic and coordination compounds, 4th ed., Wiley, New York, **1986**; pp. 282-287.

Received: November 26, 2014 **Revised: January 05, 2015** **Accepted: February 05, 2015**